

# The Electric Vehicle Torque Adaptive Drive Anti-Skid Control Based on Objective Optimization

Yingqi He

*Jiangsu Vocational College of Finance & Economics, Huai'an, 223003, China*

*School of Mechatronics and Information Engineering*

*Received July 18 2020*

*Accepted Feb 20 2021*

## Abstract

The vehicle is interfered by the lateral wind in the traditional anti-skid control method, which results in a bad anti-skid control effect of electric vehicle torque drive. For this reason, a method of torque adaptive drive anti-skid control for electric vehicle is proposed. In order to realize the driving force control of distributed driving electric vehicle, the driving motor is modeled and simplified. A battery model was established to analyze the influence of the bus voltage fluctuation on the motor torque response. The power system model is added to the existing vehicle model to complete the simulation model design of the distributed drive electric vehicle. According to the characteristics of the friction circle of the tire, the driving torque of the driving wheel is analyzed. In order to resist the influence of interference factors on vehicles during vehicle movement, through the concept of vehicle stability control, the left and right driving torque is dynamically adjusted by using the obtained ideal driving force distribution ratio of front and rear axles. The simulation results show that the proposed method can effectively increase the driving torque and improve the fitting coefficient of the driving anti-skid torque.

© 2021 Jordan Journal of Mechanical and Industrial Engineering. All rights reserved

*Keywords:* Distributed drive; Drive skid control; Driving force distribution; Dynamical system modeling;

## 1. Introduction

Automobile is an important industry of national economy. As a big country of automobile production and sales, China is not a strong country, and the technology of independent products is still weak. We should grasp the opportunity of the development of electric vehicles, achieve the leap of automotive core technology, reach the international advanced level. With its unique advantages (more controllable degrees of freedom), high-performance distributed drive electric vehicles will occupy a place in the field of electric vehicles [1].

There are many types of electric vehicle drive motors, such as dc motor, ac induction motor, permanent magnet synchronous motor and so on. The following is a brief description of its characteristics. Distributed drive electric vehicle is an electric vehicle that is powered by one or more groups of vehicle-mounted power sources to provide power to the drive motor of the wheel, so as to distribute a single controllable drive system to each wheel [2]. The so-called distributed drive electric vehicle (dev) is an electric vehicle that is powered by one or more sets of on-board power sources for each wheel's drive motor. In this way, a separate controllable drive system is distributed to each wheel. Traditional distributed drive electric vehicles can better realize the power distribution and control by taking advantage of their own structural advantages [3]. For

example, the increase and decrease of driving motor torque can be used to realize the drive anti-skid control. Driving force distribution is realized by using the advantages of independent control of driving motor and response speed. The driving anti-skid system controls the sliding rate of the driving wheel in the vicinity of the optimal sliding rate, so as to ensure that the driving wheel has the best longitudinal driving force and the ability to resist lateral interference. UOT Electric March II is an Electric car with two front wheels driven by an Electric motor [4]. The control algorithm of anti-skid drive and anti-lock braking is verified by controlling the wheel slip rate, and the concept of recognizing the wheel roll state by the driving force of the wheel is put forward. Some domestic scholars use the sliding mode control theory to achieve the drive anti-slip control. The control method of the synovial variable structure is to build the sliding mode surface by the slip rate error and the rate of error change. So it can achieve the purpose of controlling the roller slip rate. This method has good robustness, but its control principle leads to a high frequency switching of the slip rate on the synovial surface, which will cause the chattering of the drive motor and seriously affect the effect of the drive anti-slip control [5]. In order to solve the disturbance caused by side wind and buffeting of driving motor in the traditional anti-skid control method. An adaptive anti-skid control method for electric vehicle torque based on objective optimization is proposed. The effectiveness of the proposed method is verified by experiments.

\* Corresponding author e-mail: yingqi\_he@126.com.

## 2. Electric vehicle torque adaptive drive skid control

### 2.1. Objective optimization of power control algorithm

Based on the driving force control of distributed driving electric vehicles, the problem of the friction coefficient mismatch between the tire and the road caused by the torque of the driving motor and the slip of the driving wheel is studied. Under the condition of studying the driver's longitudinal intention, the car has the biggest problem of resisting lateral interference, that is, the problem of the driving force and ideal distribution between the front axle of the distributed drive electric vehicle [6]. In order to carry out research, firstly, an equivalent dynamic system model of distributed drive EV is established. Through this model, a model is sought to reflect the torque response characteristics of the motor. It can reflect the torque response caused by the battery bus voltage fluctuation problem. And the required model can meet the requirements of real-time simulation to prepare for the rapid prototyping of control algorithms in the future. In the distributed driving ev power system, the performance of the battery directly determines the performance of the vehicle [7]. Therefore, in the electric vehicle simulation, the battery model is an important link, it is very necessary to study the battery comprehensively and systematically. But the electrochemical reaction process of the battery is extremely complicated. It involves multidisciplinary fields, such as chemistry, electricity, heat, especially in the charging and discharging process, and all the performance parameters of the battery. For example, electromotive force and internal resistance, state of charge, Coulomb efficiency, self-discharge rate, and temperature, etc. can all affect each other, and there is a complicated relationship [8]. In this paper, the influence of bus voltage fluctuation on motor torque response is mainly concerned with distributed electric vehicle driving, so only a simplified internal resistance model is established. Although the internal resistance model is simple, it can reflect the basic characteristics of battery charging and discharging process, such as bus voltage fluctuation, the influence of temperature on the internal resistance, and the change of battery charge. This model is simple, universal, and convenient for simulation [9]. The following figure is the schematic diagram of the internal resistance model of the battery.

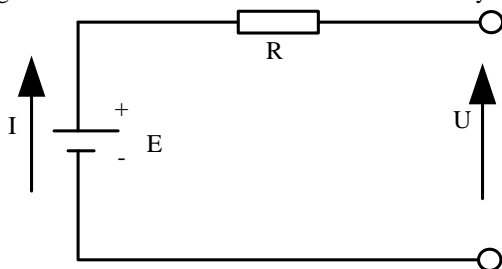


Figure 1. Internal resistance model of battery

In the vehicle model, the road adhesion coefficient is an important parameter to calculate the tire. The road adhesion coefficient where the wheels are located will change with the vehicle's track. In order to adapt to the change of the road adhesion coefficient with the track. This paper also models the road input, the idea of which is to set the road adhesion and the coordinate range [10]. When the center of mass of the wheel moves to this coordinate, the road adhesion input model will output the adhesion coefficient under the current road surface as a parameter to calculate

the current tire force. This paper illustrates how to use the road adhesion input model by taking the docking road as an example. The simplified internal resistance model simplifies the battery into the series of voltage source and internal resistance, and its basic voltage balance equation is as follows:

$$E = RI + U \quad (1)$$

where  $E$  is the electromotive force of the battery,  $R$  is the internal resistance of the battery,  $I$  is the current, and  $U$  is the bus voltage of the battery. Battery electromotive force  $E$  is determined by temperature  $T_{\text{ess}}$  and battery charge  $\text{Soc}$ , and its functional expression is:

$$\Delta E = \sum E / f(\text{Soc}, T_{\text{ess}}) \times p \quad (2)$$

The internal resistance  $R$  of the battery is determined by the battery temperature  $T_{\text{ess}}$ , the battery charge  $\text{Soc}$  and the demand power  $p$ . The functional expression is as follows:

$$R = \prod \lim_{x \rightarrow \infty} \frac{\|\Delta E - E\|}{2f(\text{soc}, \text{tess})} \quad (3)$$

where is the  $f(p)$  lookup table function. Then the power balance equation of the battery can be further obtained:

$$I = \frac{R^2 + EP_{\text{lim}}}{2E} \quad (4)$$

where,  $P_{\text{lim}}$  is the charging and discharging power of the battery after power limitation. The charging and discharging current of the battery can be simplified as follows:

$$\Delta I = \iint \frac{0.5(UR^2 + 2EP_{\text{lim}})}{2R + E} \quad (5)$$

As an emerging form of automobile, distributed drive electric vehicle has its unique advantages and many theoretical problems have not been solved. The state has carried out major basic project research (research on key basic issues of high-performance distributed drive electric vehicles) to provide theoretical support for the development of distributed drive electric vehicles. This research is not only of great significance to social environment and resource issues, but also a major strategic demand for national development [11]. The research is carried out from the two directions of driving anti-skid and driving force distribution. In the aspect of driving anti-skid control, firstly, the basic principle of driving anti-skid control and the estimation of reference speed are studied in detail, and finally, the driving anti-skid control logic for distributed driving electric vehicles is designed [12]. The distribution of driving force of distributed driving electric vehicles is divided into two parts: one is the ideal distribution of driving force in front and rear axle; the other is the dynamic adjustment of driving force from left to right. The distribution of driving force front and rear axle is a method to ensure the maximum lateral force allowance while ensuring the longitudinal acceleration of the vehicle. Dynamic adjustment of driving force from left to right is to dynamically adjust the driving torque from left to right based on the ideal distribution of driving force of front and rear axles to ensure the lateral stability of the vehicle [13]. Due to the minimum operating current limitation in the real battery system, when the battery charging current is recorded as a negative value, the minimum operating current of the battery is the maximum charging current. In order to prevent the charging current from being too large, the minimum current needs to be limited in the model. In

the actual  $e_v$ , due to the road condition or the driver, the power of the driving motor is often greater than the maximum power provided by the battery [14]. In order to be closer to the actual physical system, the model limits the external power demand. When the demand power of each driving wheel is greater than the maximum discharge power of the battery, the discharge power of the battery is limited.

2.2. Modeling of auto adaptive drive anti-skid control system

The longitudinal driving force of the vehicle is provided by the interaction between the tire and the ground. The adhesion coefficient of the road surface directly affects the longitudinal driving force, and the adhesion coefficient of the road surface has a nonlinear relationship with the slip rate of the vehicle. Through many experiments, the researchers proved that when the vehicle wheel slip rate is within a certain range, the maximum road use adhesion coefficient can be obtained. When the modified rotational slip rate becomes the optimal slip rate, the vehicle can obtain the maximum driving and braking force [15]. The larger driving force and braking force can guarantee the vehicle's handling stability and dynamic performance, so the optimal slip rate can be obtained and controlled in the optimal range, which can improve the vehicle performance. In order to make the magnetic flux density generated by PMSM close to sinusoidal distribution, the rotor magnetic steel is designed as a parabola [16]. In order to eliminate harmonic magnetomotive force, the stator windings are connected with a star. When the stator winding is connected with three-phase sinusoidal alternating current, the stator winding will generate a rotating magnetic field. The rotating

magnetic field and the constant magnetic field generated by the permanent magnets of the rotor will influence each other to push the rotor to rotate. According to the above working principle of permanent magnet synchronous motor, it can be known that as long as the phase and frequency of three-phase sinusoidal ac power supply of stator winding are changed, the speed and position of the rotor can be controlled [17]. Fuzzy control is a control method based on fuzzy mathematical theory, which represents control variables by fuzzy sets. By refining human thinking and logical reasoning methods, human experience rules are transformed into reasoning rules of logical operations, and then the controller ACTS on the control object to achieve the control effect on the controlled object [18]. In the simulation control system, the most commonly used control method is PID control, its control system principle block diagram is shown in the figure.

PID control belongs to A linear control method [19], which constitutes the control deviation according to the given target value  $r(t)$  and the actual output value  $e(t)$ , namely  $e(t) = r(t) - y(t)$ . Then carry out proportional, integral and differential calculation on the control deviation  $e(t)$ , and then add up the results of the three operations, and the control output  $u(t)$  of the PID controller is obtained. In the continuous time domain, the expression of PID control algorithm is as follows:

$$\lambda = \iiint \frac{y(t)}{2e(t) + r(t)} - 1 \tag{6}$$

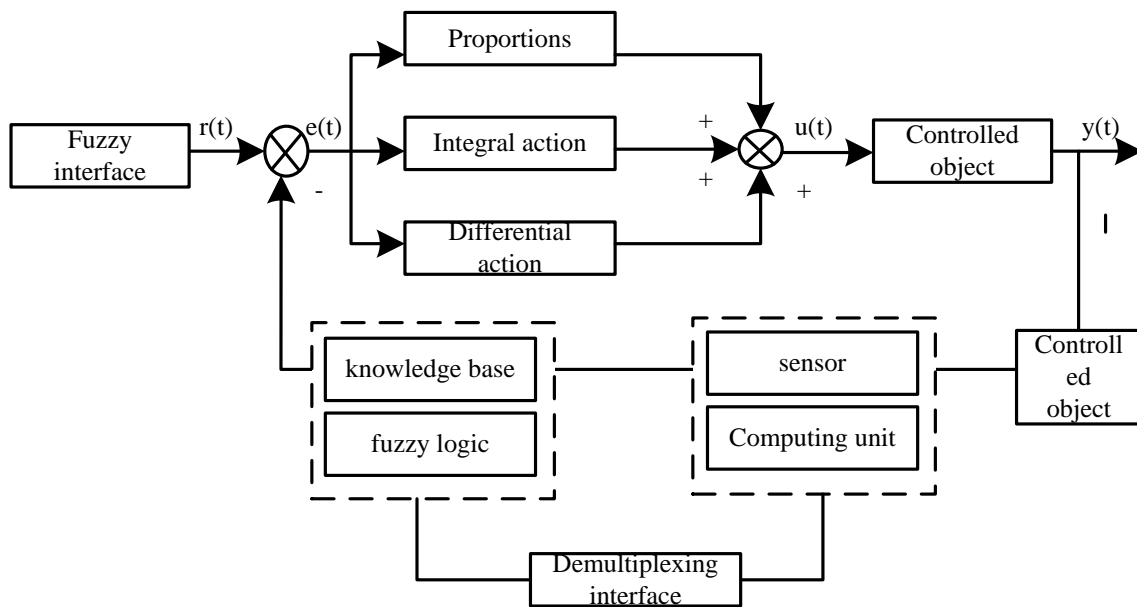
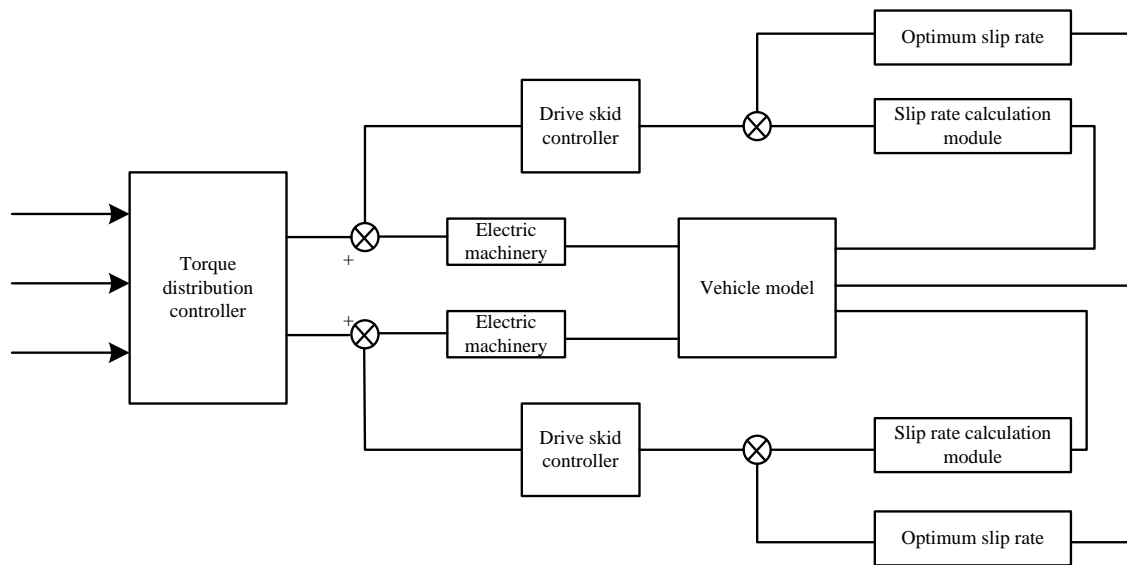


Figure 2. Schematic diagram of auto adaptive control system



**Figure 3.** Skid control structure of electric vehicle

As the main controlled object of the electric vehicle, the driving motor's performance directly affects the performance of the vehicle. Therefore, we need to establish the mathematical model of the motor and analyze it [20]. The motor is a complex physical system. In order to facilitate the analysis, the following assumptions are made in the modeling process:

1. The inductance of the motor is constant.
2. Ignore rotor damping.
3. The permanent magnetic field is sinusoidal.
4. The stator winding magnetic field is sinusoidal.
5. The stator windings are symmetrically distributed, and the axes differ from each other by 120 electric angles.

Based on this, the control strategy can be divided into two layers according to the function. The upper layer is the torque distribution control layer, and the lower layer is the driving anti-skid control layer [21-23]. Based on the fuzzy self-tuning PID control, the lower controller adopts the optimal sliding rate control strategy to control the sliding rate of the left and right driving wheels respectively to keep them near the optimal sliding rate. The two layers of control complement each other, which not only guarantees the stability of the vehicle when turning, but also makes full use of the adhesion coefficient of the ground, and improves the dynamic performance of the vehicle. The control structure is shown in the figure.

According to the automobile theory, when the wheel enters the state of sliding rotation during the driving process, the angular acceleration of the wheel will increase rapidly, and the sliding rate of the wheel will also increase sharply. Therefore, the angular velocity of the wheel can reflect whether the vehicle is in a state of skidding to some extent. There is an important relationship between wheel slip rate and wheel angular acceleration. Therefore, an anti-slip control algorithm based on wheel angular acceleration and reference slip rate is proposed to combine the two as the input of the controller. The observation model of wheel angular acceleration and reference slip rate is derived. The drive anti-skid control method based on the optimal slip rate

can solve the problem of excessive sliding of the drive wheel when the electric vehicle accelerates rapidly to a certain extent. However, there are also some defects, such as drive torque fluctuations, speed detection difficulties. In order to solve the above problems, a driving anti-skid control method based on wheel angular acceleration and reference slip rate is proposed. This control method can monitor the wheel angular acceleration in real time and predict the change of slip rate according to the positive and negative of the angular acceleration. The reference slip rate is used to estimate the speed. Therefore, it can effectively make up for the shortcomings of the control method based on the optimal slip rate.

### 2.3. Realization of anti-skid control of electric vehicle drive

Vehicle drive skid control system (ASR) belongs to vehicle traction control system (TCS), which is a kind of vehicle active safety control. Driving anti-skid control can control the wheel slip rate within a reasonable range, so that the wheels can obtain greater adhesion. It can prevent the vehicle from over-driving the wheels to slip during starting or accelerating, resulting in reduced longitudinal driving force and vehicle side adhesion. The drive skid control can effectively improve the stability and safety of the vehicle. With the development of pure electric vehicle (ev) has become a hot topic among researchers from all over the world, the research and development of anti-skid driving system has attracted more and more attention. One of the most important parts of the automobile drive anti-skid control system is the control method of the drive anti-skid system. At present, the logic threshold control method is used in most of the widely used drive anti-skid products. The logic threshold control method does not involve specific mathematical model, avoids complex theoretical calculation and analysis, and simplifies the controller design process. However, the controller threshold value can only be obtained through repeated tests, which is largely

dependent on experience and has no sufficient theoretical basis. In addition, the vehicle's dynamic characteristics and road attachment conditions will change in real time during actual operations. Therefore, the robustness of logic limit control is not enough to satisfy the control effect of the vehicle under different conditions. The torque control of each wheel of distributed drive ev is independent of each other, so its driving force distribution scheme is varied. Also, since the driving force of each wheel is independently controllable, there is no need to add additional equipment for the driving force control of each driving wheel, and the driving anti-skid control system can be used at a lower cost. The purpose of this paper is to study a method of reasonably distributing the driving force of the front and rear axles to drive the wheels under the condition of ensuring the longitudinal force. So that the vehicle has the largest lateral force margin during driving. During driving, to resist lateral interference and ensure the lateral stability of the vehicle during driving. In actual electric vehicle systems, there are various forms of interference. For example, the drive motor drive torque expression error interference (the so-called drive motor drive torque expression error interference, such as a torque command of 100 N/m from the upper control system). And the actual output torque of the drive motor is 80 N/m, and yaw operation deviation is likely to occur. With the help of ESP, a driving force control algorithm for dynamic adjustment of left and right driving forces is designed to make the car more stable during driving. The relationship between slip rate and road adhesion coefficient can be seen that with the change of tire slip rate, both longitudinal and lateral road adhesion will change. In order to ensure a good longitudinal adhesion, lateral adhesion and not too much loss, it is necessary to control the tire slip rate in a certain range. The basic idea of logic threshold control is to control the tire slip rate between  $S$  ( $S$  is the specified slip rate range of vehicle tires). To ensure that the car tires have greater longitudinal adhesion during driving. In order to ensure the driving dynamic performance, there must be greater lateral adhesion to ensure the steering of the vehicle and prevent sideslip.

As can be seen from Fig. 4, the optimal adhesion characteristics of tires can be guaranteed as long as the control of wheel slip rate is maintained. Vehicle dynamics is mainly to study the vehicle motion under various working conditions, including longitudinal motion, lateral motion and vertical motion. Longitudinal dynamics mainly studies the dynamic response of vehicles in the longitudinal direction under driving and braking conditions. Lateral dynamics mainly studies the dynamic response of the vehicle in the lateral direction and the lateral characteristics of tires under the influence of steering wheel Angle input or crosswind. Vertical dynamics studies the dynamic response of vehicles in vertical direction, and mainly analyzes the vibration, pitch and other motion of vehicles under the excitation of road surface. An effective tool to study the dynamic characteristics of vehicles under various operating conditions is to establish mathematical models of vehicles. The mathematical model can express the motion state of the vehicle in the form of mathematical equation, and further study the vehicle dynamics. CarSim software was used to

parameterize the vehicle model, including rolling resistance and air resistance characteristics of the vehicle, yaw moment of inertia, nonlinear tire sidetracking characteristics, steering gear ratio and other parameters [24]. The formula of longitudinal slip rate of wheels in the process of automobile driving is as follows:

$$S = \frac{R - \lambda}{2\Delta E + \Delta I} \times 100\% \quad (7)$$

It can be seen from the formula that the wheel slip rate is determined by the vehicle speed and wheel speed. As long as the wheel speed is controlled, the purpose of controlling the wheel slip rate can be achieved. When a car is running, almost all external forces, except air resistance, act on the tires through the ground. The motion characteristics of the vehicle are closely related to the forces exerted on the tires, so the tire model has a great impact on the accuracy and reliability of the simulation results. Further calculate the anti-slip control program, and the iterative process is as follows:

1. Specify the population size, that is, how many individuals are in each generation. Using a large population scale, the genetic algorithm can search the space more thoroughly, but will make the genetic algorithm run slowly. Here, the initial population scale is set to 200. That is to seek the optimal solution of tire model parameters among 200 vectors.
2. The genetic algorithm iterates with the mechanism of superior and slight elimination to eliminate the individuals with small fitness and select the high-quality individuals with large fitness for reproduction. The best individual is selected through a sorting algorithm. This sorting algorithm measures the pros and cons of individuals based on the order of individual fitness values rather than the size of individual fitness. Thereby eliminating the influence of original fitness.
3. High quality individuals produce offspring through crossover and mutation. Crossover is when two good individuals swap genes at one point or more to produce a new individual. The probability of crossing is 0.85. Variation is to create variation children by changing individuals in a population with a small random number, so that the genetic algorithm can search a wider space and select uniform variation with a probability of 0.010.
4. Repeat 2 and 3 steps to carry out iterative calculation on the population, meet the cut-off condition, and get the optimal solution.

At present, the commonly used tire models are divided into empirical model, theoretical model and semi-empirical model. The semi-empirical model is based on theoretical research and combined with data. It has the advantages of other two models and is more accurate. The vehicle anti-skid (ASR) control system adjusts the torque of the driving wheels through appropriate control algorithms and control strategies. In this way, the slip ratio of the driving wheels is kept within the optimum range, thereby ensuring a vehicle with the best driving capability. In this paper, the anti-skid control algorithm and strategy of four-wheel drive vehicle are studied, as shown in Figure 5.

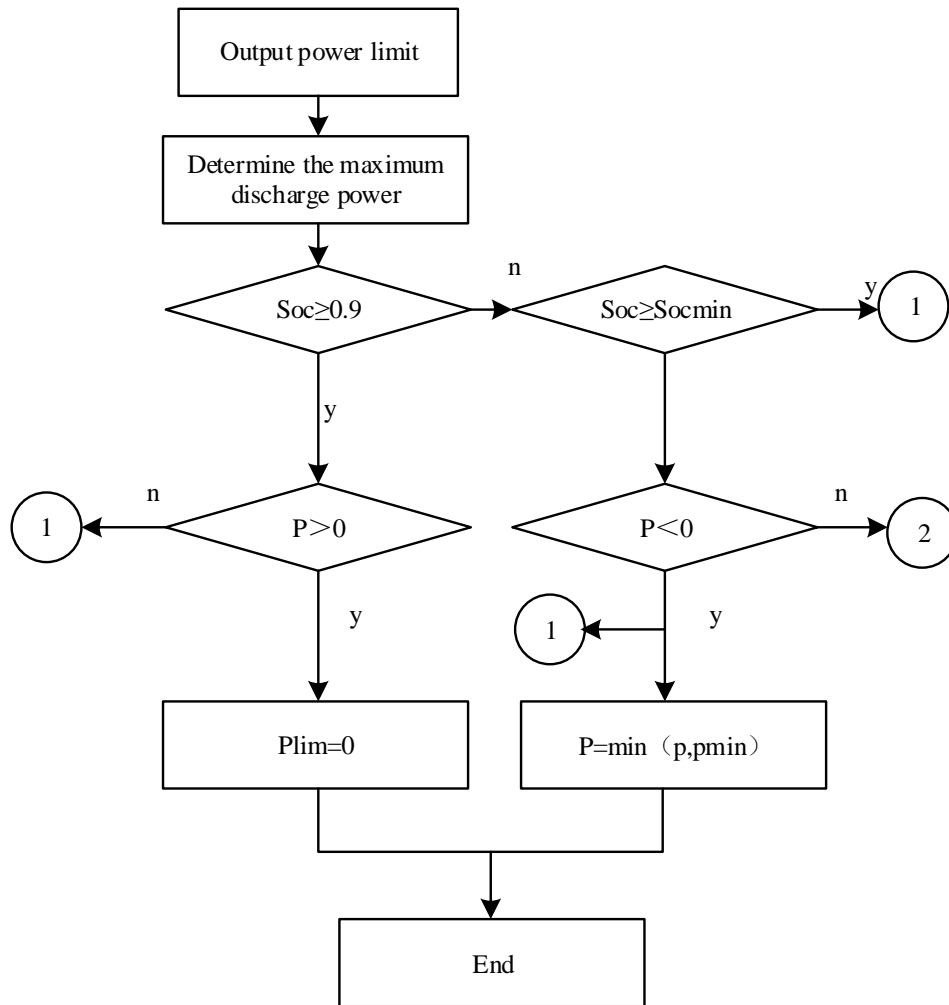


Figure 4. Anti-skid control flow of electric vehicle drive

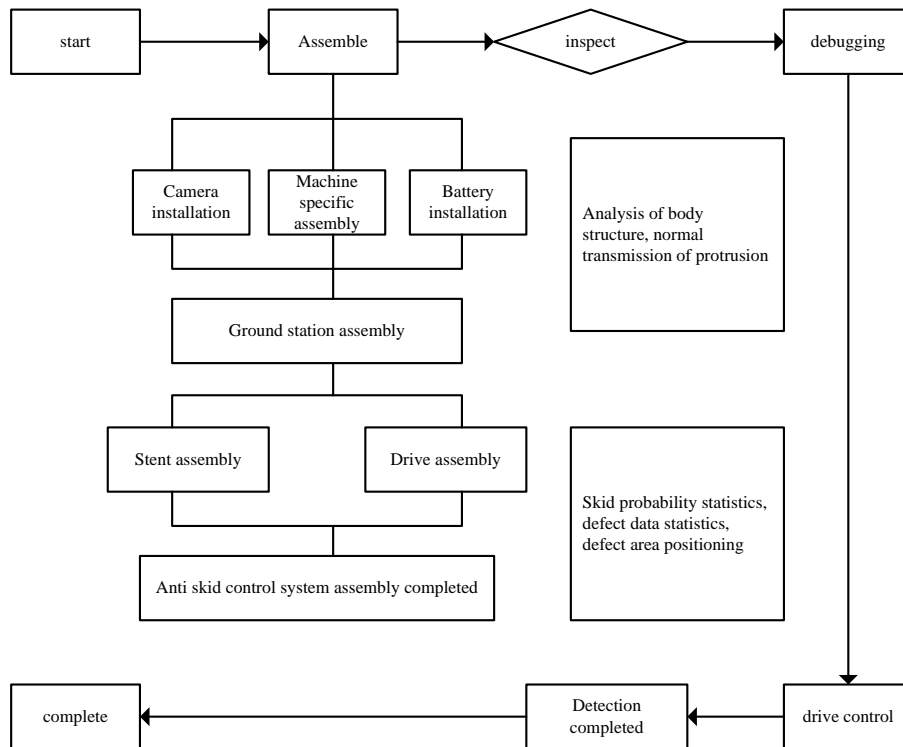


Figure 5. Anti-skid control mode of electric vehicle drive

Based on the sliding mode variable structure control algorithm, the optimal driving torque of the vehicle is determined in real time according to the speed of the vehicle and the sliding speed of the driving wheel. The torque allocation strategy is based on the fuzzy control algorithm, which comprehensively considers the driving speed, battery SOC and demand torque, and reasonably distributes the torque of engine, motor and wheel-yi motor on the principle of high engine efficiency and good economy. Both the sliding mode variable structure control and the fuzzy control have strong robustness. It does not need to establish an accurate mathematical model of the controlled system, and it has little dependence on the system.

### 3. Analysis of simulation results

#### 3.1. Simulation design

Due to the real motion of the vehicle system there will be many unpredictable interference factors, such as lateral wind interference, driving motor, driving torque expression error interference. In order to resist the influence of interference factors on vehicles during vehicle movement, with the help of the concept of vehicle stability control, the left and right driving torque is dynamically adjusted by using the obtained ideal driving force distribution ratio of front and rear axles, and the theoretical algorithm is simulated and verified. Simulink was used to build ideal vehicle model. Simulink is a software package used to model, simulate and analyze dynamic systems. It supports linear and nonlinear systems, continuous and discrete time models, or a mixture of the two. In the vehicle simulation system, the ABS controller reads the wheel speed signal from the wheel speed sensor. According to the internal

algorithm, it sends out the pressure increase, hold pressure and pressure reduction signals that make the brake actuate. This signal is input to the computer through the interface circuit and converted into a signal that can be recognized by the vehicle model. The vehicle model accepts inputted vehicle parameters such as vehicle mass, initial braking speed, etc., to simulate the operating state of the vehicle under ABS control. But the ideal model would ignore some degree of freedom, wind resistance, road surface and other factors. Therefore, this kind of simulation platform cannot well verify the control effect of the controller under the limit condition. A general electric vehicle co-simulation platform was established by using Simulink and Carsim software, and a simulation platform for pure electric vehicle drive control system was designed according to the requirements. Its structure is shown in the figure. The control strategy and motor model are built in Simulink software, and the vehicle dynamics model is built in CarSim software. The two can form a seamless connection. Based on this, the vehicle drive anti-skid control simulation platform based on Simulink is demonstrated as follows:

The vehicle test platform developed in this paper adopts the independent drive scheme of the rear wheel double motor. Considering cost, design difficulty, feasibility and other factors according to the actual requirements, the vehicle design mainly aims at the power and range. The vehicle design objectives are summarized as follows: Power: maximum speed >50 km/h; 100 km acceleration 5 s; Maximum climbing grade 10%;

Range: >30 km on a single charge;

Control system: it is a general configurable control platform which can quickly realize the modification of driving control strategy and realize the acquisition and processing of sensor signals.

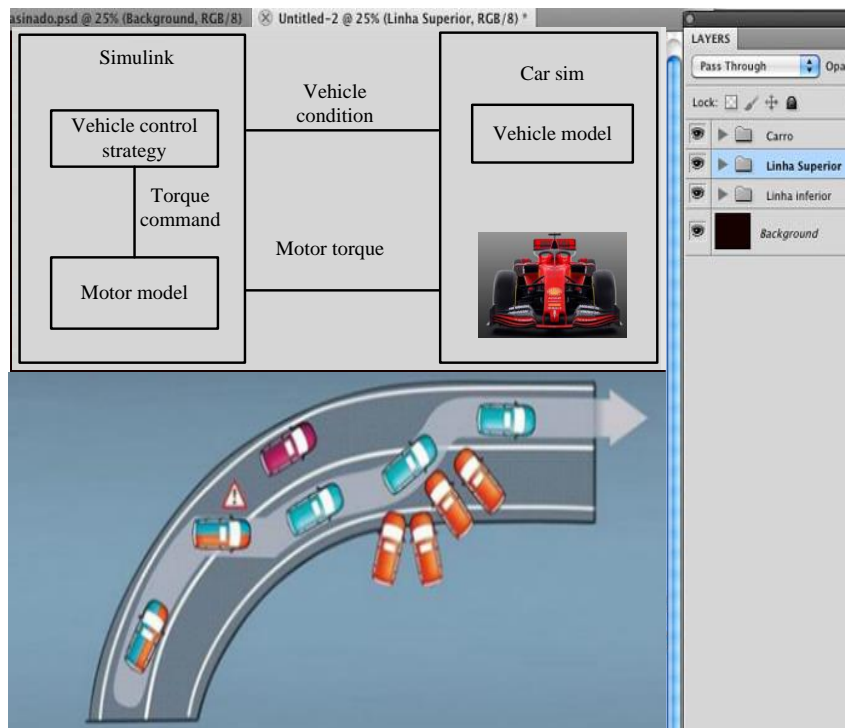


Figure 6. Simulation platform of vehicle drive anti-skid control based on Simulink

**Table 1.** Simulation parameters

Parameter	numerical value	Units
Vehicle quality	350	Kg
Length × width × height	160*120*180	mm
Wheelbase	1600	mm
Track width (front / rear)	1240/1260	Mm
Reduction ratio of reducer	4.2	-
Minimum ground clearance	80	mm
Centroid height	320	mm
Distance from center of mass to front / rear axle	860	mm
Yaw moment of inertia	221.62	Kg/m <sup>2</sup>
Rated power	36	Kw
peak power	84	Kw
Torque setting	80	Nm
Peak torque	140-160	Nm
Maximum speed	300-320	Rpm
input voltage	300-330	v
Rated current	560-590	A
peak current	8000	A
Rated torque	5.4	Nm
Maximum torque	12000	Nm
Maximum input speed	3.6	Rpm
Quality	2.75	KG
Nominal capacity	4.6	mAH
Rated voltage	70	V
Discharge cut-off voltage	160	V
Charging cut-off voltage	280	V
Maximum continuous charging current	16	A
Maximum instantaneous charging current	≤0.6	A
Maximum continuous discharge current	264±0.2	A
Maximum continuous discharge rate	12-3600	C
internal resistance	3*360	m
Weight	3	kg
Operating temperature (charging and discharging)	0-35/-16-20	°C

Combined with the data in the above table, CRIO vehicle controller is further used for experiments. Its main functions include: collecting and processing the driver's driving intention, vehicle status and other signals, the calculation of vehicle drive control strategy, and sending the command signals such as torque output, mode and running state to the motor driver through the communication association. As the underlying controller, the main functions of the motor driver include: receiving the command signal of the vehicle controller, collecting the actual torque, speed, current, temperature and other signals of the drive motor, and feeding them back to the vehicle controller through the communication protocol. The sensor system is responsible for collecting the driver's driving intention and vehicle status signals, mainly including: accelerator pedal sensor, brake pedal sensor, steering wheel Angle sensor, triaxial

acceleration sensor, wheel speed sensor, etc. CRIO vehicle controller input interface definition and each signal form are shown in Table 2.

**Table 2.** Output signal acquisition of vehicle controller

Input quantity	Function description	Signal source	Signal form
Accelerator pedal signal	Expected torque of the whole vehicle	Accelerator pedal sensor	0.5-4.5 v
Brake pedal signal	Brake control signal	Brake pedal sensor	0.5-4.5 v
Steering wheel angle signal	Check steering wheel angle	steering wheel angle sensor	Can communication protocol
Motor speed times	Detection of motor speed	Motor driver motor driver	Can communication protocol
Motor torque signal	Test motor torque	Motor driver motor driver	Can communication protocol
Yaw rate multiple	Obtain yaw rate	Triaxial acceleration sensor	0-5 V voltage
Longitudinal acceleration signal	Obtain longitudinal acceleration	Triaxial acceleration sensor	1.2 ~ 1.2 V
Lateral acceleration signal	Obtain lateral acceleration	Triaxial acceleration sensor	1.2~ 1.2 v
Wheel speed signal	Get wheel speed	Wheel speed sensor	0~5 V voltage
Reserved interface	Follow up signal supplement	-	-

### 3.2. The simulation results

#### 3.2.1. Drive skid - proof buckle notification rule detection

According to practical experience and simulation results, in order to prevent the wheel from over-sliding, the wheel angular acceleration should be kept within the range of PM, and the slip rate should be kept within the range of PS. Therefore, the design of fuzzy inference rules is shown in the table, with a total of 28 fuzzy inference rules.

**Table 3.** detection results of the notification rules of the adaptive drive skid buckle

Rule	Input		Output
	Wheel angular acceleration	Slip ratio	Torque output
1	PS	NB	PS
2	ZE	NB	ZE
3	PM	NB	PM
4	PB	NB	PB
5	ZE	NM	PS
6	PS	NM	ZE
7	ZE	NM	PM
8	PB	NS	PB
9	PB	NS	PS
10	PS	NS	ZE
11	PM	NB	PM
12	PM	NM	PB

In Table 3, P is the initial value of actual acceleration, PB is the range of actual acceleration value, PM is the reasonable range of acceleration, PS is the predicted range of acceleration, N is the initial value of slip rate, and NB is the range of actual slip rate. NM is the reasonable range of slip rate, and NS is the predicted range of slip rate. ZE is the reasonable range of torque output. It is the key of the

research to simulate the road running condition of the vehicle when the vehicle starts or accelerates rapidly, when the vehicle starts with the maximum output torque. In the simulation, the steering wheel angle was set to remain at zero. The road adhesion coefficient is 0.85. The driving torque of the vehicle within 15s under DRI reaches the maximum 70Nm dimension command. The vehicle continues to accelerate until the steering wheel is overloaded. The initial speed of the vehicle is set to 20 m/s, maintaining a uniform speed, the front wheel Angle reaches 60 at 0.5 s and remains unchanged, and the accelerator pedal opening remains unchanged. The road adhesion coefficient is set to 0.2. This condition is simulated when the driver suddenly encountered in front of the obstacle, there is no time to brake, to suddenly hit the direction of the operation.

### 3.2.2. Comparison of front and rear drive wheel slip rate

Based on the above, the simulation was conducted, and the test results were recorded. The specific results are shown in Figure 7:

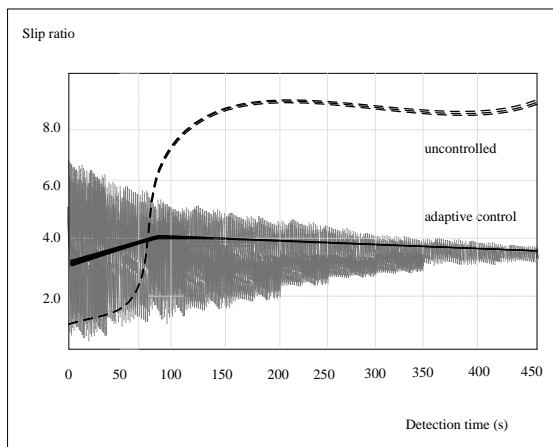


**Figure 7.** Detection of front and rear driving wheel slip rate of electric vehicle

As can be seen from Fig. 7, the dotted line is the slip rate of the driving wheel under the control of non-skid control. During acceleration, the slip rate of the driving wheel rapidly increases to 0.9, reaching the maximum value, and the wheel overrolls. The solid line is the curve of the sliding rate of the driving wheel after the driving anti-skid control. It can be seen from the figure that under the driving anti-skid control, the sliding rate of the driving wheel can be effectively controlled within the optimal sliding rate of 0.25 or so, and the maximum sliding rate does not exceed 0.3. Under the driving anti-slip control, the yaw velocity fluctuates greatly because of the additional yaw moment. Under the drive anti-slip control based on objective optimization, the yaw velocity is basically coincident with the ideal value, and the response is quick, and the overshoot is small. Under the drive anti-slip control, the maximum value of the center of mass side Angle is -0.16 rad, which fluctuates seriously and does not reach the steady-state value within 10 s. Under the drive anti-slip control based on the objective optimization control, the maximum value of the center of mass side Angle is -0.018 rad, and the response is rapid, and the steady-state value is reached at 0.5 s. It can be seen from the above analysis that the drive anti-skid control can control the slip rate of the drive wheel within the

ideal range, and effectively control the excessive roll of the wheel. But it will produce extra yaw moment, increase the value of yaw angle, speed and center of mass yaw angle. And the fluctuation will become larger, which will damage the lateral stability of the vehicle. The anti-skid control based on objective optimization, by optimizing the left and right driving torque distribution and offsetting the additional yaw torque, ensures the lateral stability of the vehicle while controlling the driving wheel slip rate.

### 3.2.3. Comparison of fitting coefficient of driving anti-skid torque

In order to further verify the anti-skid control effect of the designed method for electric vehicle driving, the anti-skid torque fitting coefficient is detected, and the detection result is shown in Fig. 8.

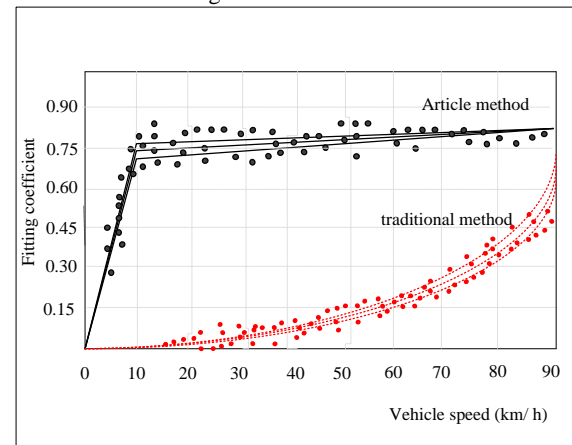


**Figure 8.** Test of torque fitting coefficient of driving skid resistance

The fitting coefficient of driving anti-skid torque determines the anti-skid control effect. The larger the coefficient is, the better the anti-skid control effect will be. Fig. 8 shows that the fitting coefficients of the driving anti-skid torque are different at different speeds. When the vehicle speed is low and the vehicle speed is 10 km/h, the fitting coefficient of the driving anti-skid torque of the traditional method is 0.01, while the fitting coefficient of the driving anti-skid torque of this method is 0.71. When the vehicle speed increases to 50 km/h, the fitting coefficient of the traditional method is 0.14, while the fitting coefficient of the driving anti-skid torque of this method is 0.75. The fitting coefficient of the driving anti-skid torque is always large, which indicates that the torque anti-skid control in this paper is effective.

### 3.2.4. Driving moment contrast

In order to verify the effect of driving torque control of the method in this paper, the anti-skid control method with energy consumption optimization and the anti-skid feedback control method with driving anti-skid control with target optimization are compared. The results are shown in Fig. 9.

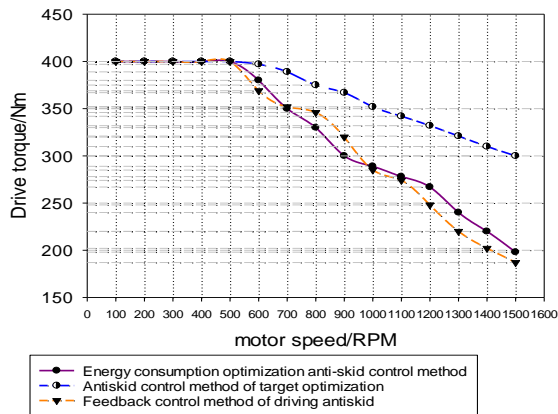


Figure 9. Driving torque control effect

Fig. 9 shows that when the motor speed of electric vehicles is within 0-500 RPM, the driving torque of the three methods is kept at 400 Nm. When the motor speed of the car exceeds 500 RPM and reaches 600 RPM, the driving torque of the energy consumption optimization anti-skid control method is 380 Nm. The driving torque of the anti-skid control method for driving is 369 Nm, and the torque of the target optimized anti-skid control method is 397 Nm. When the speed of the car motor reaches 1300 RPM, the energy consumption of the anti-skid control method with a driving torque of 240 Nm is optimized. The driving torque feedback control method is 220 Nm. The goal is to optimize the anti-skid control method of 321 Nm driving torque. This method can effectively increase the driving torque when the motor speed is too high and improve the anti-skid control effect.

#### 4. Conclusion

In order to control the torque of electric vehicle, this paper designs a method of anti-skid control of vehicle torque based on objective optimization. The wheel angular acceleration and the reference slip rate are used as the two inputs of the fuzzy controller, and the torque of the driving motor is used as the output of the fuzzy controller. This controller can predict the change direction of tire slip rate according to the signal of wheel angular acceleration and prevent the fluctuation of driving torque caused by sudden change of motor torque. The wheel angular acceleration and reference slip rate were estimated by motor torque signal and wheel angular velocity signal. The following conclusions are drawn from the experiment:

1. The fitting coefficient of the driving anti-skid torque is always large, and the torque anti-skid control effect is better. When the vehicle speed increases to 50 km/h, the fitting coefficient of the traditional method is 0.14, while the fitting coefficient of the method in this paper is 0.75.
2. The method in this paper can effectively control the torque of electric vehicles against skid. When the motor speed reaches 1300 RPM, the driving torque of the method can still reach 321 Nm.

#### References

- [1] Andersen KH, Bertelsen M, Zanini L, et al. Optimization of moderators and beam extraction at the ESS. *Journal of Applied Crystallography*, 2018, 51(2):264-281.
- [2] Pinson RM, Lu P. Trajectory design employing convex optimization for landing on irregularly shaped asteroids. *Journal of Guidance Control and Dynamics*, 2018, 41(6):1-14.
- [3] Ekanayake S, Dutta R, Rahman MF, et al. Direct torque and flux control of interior permanent magnet synchronous machine in deep flux-weakening region. *Iet Electric Power Applications*, 2018, 12(1):98-105.
- [4] Otsuka T, Kuroiwa Y, Sato K, et al. Use of mixer torque rheometer to clarify the relationship between the kneading states of wet mass and the dissolution of final product in high shear granulation. *Chemical & Pharmaceutical Bulletin*, 2018, 66(5):554-561.
- [5] Oene MMV, Ha S, Jager T, et al. Quantifying the precision of single-molecule torque and twist measurements using Allan variance. *Biophysical Journal*, 2018, 114(8):1970-1979.
- [6] Janzen NR, Hight RE, Patel DS, et al. Estimation of critical end-test torque using neuromuscular electrical stimulation of the quadriceps in humans. *European Journal of Applied Physiology*, 2018, 118(2):1-8.
- [7] Liang T, Wang XJ, Luo LQ. Torque adaptive allocation control of four wheel distributed drive electric vehicle. *Computer Simulation*, 2018, 035(012):111-116.
- [8] Jiang T, Geng C, Xue QC, Zhang X. Torque distribution strategy of front and rear axle independent drive electric vehicle based on energy consumption optimization. *Engineering of Surveying and Mapping*, 2019, 43(05):102-109.
- [9] Tang QD, Ge X, Liu YC, et al. An improved switching-table-based DTC strategy for the post-fault three-level NPC inverter-fed induction motor drives. *Iet Electric Power Applications*, 2018, 12(1):71-80.
- [10] Siracusano G, Tomasello R, D'Aquino M, et al. Description of statistical switching in perpendicular STT-MRAM within an analytical and numerical micromagnetic framework. *IEEE Transactions on Magnetics*, 2018, 54(5):1-10.
- [11] Ende MVD, Chen JY, Ampuero J, et al. A comparison between rate-and-state friction and microphysical models, based on numerical simulations of fault slip. *Tectonophysics*, 2018, 733:273-295.
- [12] Zhou XP, Chen YD, Zhou, LM, et al. Power coordinated control method with frequency support capability for hybrid single/three-phase microgrid. *Iet Generation Transmission & Distribution*, 2018, 12(10):2397-2405.
- [13] Xiao J, Hu C, Ouyang G, et al. Impacts of oil implied volatility shocks on stock implied volatility in China: Empirical evidence from a quantile regression approach. *Energy Economics*, 2019, 80(5):297-309.
- [14] Wen F, Zhao Y, Zhang M, et al. Forecasting realized volatility of crude oil futures with equity market uncertainty. *Applied Economics*, 2019, 51(59):6411-6427.
- [15] Jiang DS, Correa-Gallegos D, Christ S, et al. Two succeeding fibroblastic lineages drive dermal development and the transition from regeneration to scarring. *Nature Cell Biology*, 2018, 20(4):422-431.
- [16] Linn, J, Wang, Z, Xie, L. The long-run effects of housing location on travel behavior: Evidence from China's housing reform. *Canadian Journal of Chemistry*, 2018, 49(6):695-702.
- [17] Caldwell KB, Boyer RHW. Bicycle commuting in an automobile-dominated city: how individuals become and remain bike commuters in Charlotte, North Carolina. *Transportation*, 2018, 47(4):1-22.
- [18] Othman RNFKR, Zuki NAM, Ahmad SRC, et al. Modelling of torque and speed characterisation of double stator slotted

- rotor brushless DC motor. *Iet Electric Power Applications*, 2018, 12(1):106-113
- [19] Hsu CH. Fractional Order PID Control for Reduction of Vibration and Noise on Induction Motor. *IEEE Transactions on Magnetics*, 2019, (99):1-7.
- [20] Trancho E, Ibarra E, Arias A, et al. PM-assisted synchronous reluctance machine flux weakening control for EV and HEV applications. *IEEE Transactions on Industrial Electronics*, 2018, 65(4):2986-2995.
- [21] Li J. Distributed multi-level inventory algorithms for automotive maintenance spare parts based on centralized control model. *Jordan Journal of Mechanical and Industrial Engineering*, 2020, 14(1):89-99.
- [22] Rahimi M, Fazlollahtabar H. Optimization of a closed loop green supply chain using particle swarm and genetic algorithms. *Jordan Journal of Mechanical and Industrial Engineering*, 2018, 12(2):77-91.
- [23] Gao H, Sun Z, Tao L, et al. Effect of fiber modulus on natural frequency of composite automobile drive shaft. *Fiber Reinforced Plastics/Composites*, 2018, (05):58-63.
- [24] Li Y, Deng HF, Xu X, et al. Modelling and testing of in-wheel motor drive intelligent electric vehicles based on co-simulation with Carsim/Simulink. *IET Intelligent Transport Systems*, 2019, 13(1):115-123.